INTERNATIONAL JOURNAL FOR NUMERICAL METHODS IN FLUIDS, VOL. 8, 31–53 (1988)

ENTROPY AND VORTICITY CORRECTIONS FOR TRANSONIC FLOWS

M. HAFEZ

University of California, Davis, CA 95616, U.S.A.

AND

D. LOVELL

Flow Research Company, Kent, WA, U.S.A.

SUMMARY

Different models for inviscid transonic flows are examined. The common assumptions that the flow is isentropic and irrotational are critically evaluated. Entropy and vorticity correction procedures for potential and stream function formulations are presented, together with the details of the treatment of shocks and wakes, and drag and lift calculations. The non-uniqueness problem of the potential formulation is studied using different artificial viscosity forms. Numerical results are compared with Euler solutions.

KEY WORDS Non-isentropic transonic flows Non-uniqueness Stream function solutions

INTRODUCTION

In 1970, Magnus and Yoshihara[1] reported transonic calculations using a Lax–Wendroff scheme with augmented viscosity where shocks were captured. At the same time, Murman and Cole[2] introduced their type-dependent finite difference relaxation method for solving the transonic small-disturbance potential equation and it was demonstrated that some comparable results can be obtained with this simple model, which is much less expensive. Later, Murman[3] introduced his fully conservative scheme and Jameson[4] extended Murman's work to solve the full potential equation. Since then, conservative versus non-conservative calculations have been the subject of many papers. Shocks in conservative calculations are usually stronger and are placed further downstream compared with the non-conservative ones. Since conservative calculations, combined with boundary layer codes, may lead to artificial separation, some engineers prefer to use non-conservative codes. It was noticed that Euler results lie in between the conservative and the non-conservative potential calculations. In fact, a linear combination of both is closer to the more exact answer. Lock[5] suggested a quasi-conservative scheme; a weighted average scheme which satisfies the Rankine–Hugoniot jump conditions. His empirical fix is useful, in particular after Steinhoff and Jameson[6] discovered that conservative potential codes produce non-unique solutions in a range of Mach numbers and angles of attack of engineering interest, while Euler and non-conservative codes do not have this problem, atleast for the same cases.[7]

Meanwhile, there has recently been distinct progress in solving the Euler equations implicitly [8,9] or explicitly.[10–12] It seems that potential codes will be replaced by Euler ones which can be made

0271–2091/88/010031–23$11·50

Received 9 April 1986
Revised 15 February 1987

efficient especially on the new computers, exploiting the advantages of vector/parallel processing.

It is still of interest, however, to fix the potential codes using more systematic methods to produce results closer to Euler solutions. By weakening the shock, there is less chance to have the non-uniqueness problem. After all, it is not clear that the steady Euler equations should have a unique solution.

In this paper, the differences between the potential formulation and Euler equations are examined. Different models including the entropy and vorticity effects are discussed. A modified potential formulation, where Rankine–Hugoniot shocks are fitted, is recommended (i.e., the vorticity downstream of a shock can be neglected, especially if shock curvature is small). A simple method to implement the entropy correction is introduced and results are compared with both existing potential and Euler solutions. (See References 13–15 for similar formulations.) On the other hand, it is shown that for isentropic models, where mass and momentum are conserved (but the flow is not isoenergetic), shocks are weak and vorticity is generated due to the variation of the total enthalpy, and the results are very close to Euler solutions.

Other models are also studied. In particular for two-dimensional and axisymmetric flows, the stream function formulation is very attractive. The entropy and vorticity effects can be easily included and, in this case, their solution is completely equivalent to Euler equations.

Finally, the non-uniqueness problems are discussed. In general, artificial viscosity and time-marching integration procedures exclude certain types of non-uniqueness, but there might be no steady state solution. In existing potential codes, the artificial viscosity is switched off in the subsonic part of the shock to produce sharp profiles. If uniform viscosity were used, converged unique solutions are obtained (with smeared shocks) for the same conditions where existing codes produce non-unique solutions.

In the following, the details are given and some numerical results are presented.

EULER EQUATIONS

The exact model of inviscid flow, namely, Euler equations, represents conservation of mass, momentum and energy. In Cartesian co-ordinates, the equations for two-dimensional flows using standard notation are

$$\rho_t + (\rho u)_x + (\rho u)_y = 0, \tag{1}$$

$$(\rho u)_t + (\rho u^2 + p)_x + (\rho uv)_y = 0, \tag{2}$$

$$(\rho v)_t + (\rho uv)_x + (\rho v^2 + p)_y = 0, \tag{3}$$

$$(\rho e)_t + (\rho uh)_x + (\rho vh)_y = 0, \tag{4}$$

where

$$e = p/(\gamma - 1)\rho + \tfrac{1}{2}q^2, \quad h = e + p/\rho.$$

For a steady flow around an aerofoil, with a uniform free stream, h is constant throughout the domain. If mass, momentum and energy are conserved, it is not possible to put a restriction on entropy or vorticity. Across a shock the entropy jump is

$$\frac{\Delta S}{R} = \frac{1}{\gamma - 1}\left[\log\left(\frac{2\gamma}{\gamma + 1}M^2 \sin^2\beta - \frac{\gamma - 1}{\gamma + 1}\right) - \gamma \log\left(\frac{(\gamma + 1)M^2 \sin^2\sigma}{(\gamma - 1)M^2 \sin^2\beta + 2}\right)\right], \tag{5}$$

where M is the Mach number of the flow upstream of the shock and β is the shock inclination. Due to the curvature of the shock, the vorticity generated is (Crocco relation)

$$\omega = p\frac{\mathrm{d}\,\Delta S/R}{\mathrm{d}\psi}. \tag{6}$$

Across the wake (contact discontinuity), the density jumps, while the pressure and the tangential velocity are continuous. At a sharp trailing edge, to have the same static pressure on the lower and upper surfaces, the flow leaves the aerofoil tangential to the surface of higher total pressure (i.e., lower entropy). It adjusts itself in a very short distance and asymptotically becomes parallel to the free stream. In the far field, downstream of the body, the pressure is uniform, but there is a variation of the speed and the density (in the direction normal to the stream) due to the vorticity. The drag can be estimated in terms of the entropy generated by shocks (Oswatitsch formula):[16]

$$D = \frac{T_\infty}{q_\infty}\int_{\text{shocks}} \rho q_\mathrm{n}\,\Delta S\,\mathrm{d}l. \tag{7}$$

To calculate the circulation in the far field (lift), the contribution from the vorticity generated by shocks should be included; in many practical cases, however, it could be neglected. Many codes are available to solve equation (1)–(4) implicitly or explicitly, where some kind of artificial viscosity is used to capture shocks.

ALTERNATIVE FORMULATIONS

If a shock-fitting procedure is used, the x and y momentum equations can be replaced by the corresponding non-conservative forms; namely, S and ω/p are constants along streamlines, with the proper jumps across shocks. The continuity and the vorticity equations in conservation form are solved for the velocity components:

$$(\rho u)_x + (\rho v)_y = 0, \tag{8}$$

$$-u_y + v_x = \omega, \tag{9}$$

where

$$\rho = \rho_i \mathrm{e}^{-\Delta S/R}, \quad \rho_i = \left(1 - \frac{\gamma-1}{2}M_\infty^2(u^2+v^2-1)\right)1/(\gamma-1),$$

$$p = p_i \mathrm{e}^{-\Delta S/R}, \quad p_i = \rho_i^\gamma/\gamma M_\infty^2.$$

The jump conditions admitted by equations (8) and (9) are

$$[\rho q_\mathrm{n}] = 0 \tag{10}$$

and

$$[q_\mathrm{t}] = 0, \tag{11}$$

where ρq_n is the flux normal to the shock and q_t is the tangential velocity. The conservation of the normal momentum is satisfied through imposing the right entropy jump. Actually, in this model, only a shock detection is needed, since once the shock position and inclination are known, ΔS and ω can be calculated from equations (5) and (6).

Equation (8) can be written in a non-conservative form. In this case, the shock must be treated as an internal boundary to satisfy the jump conditions. The velocity components u and v are obtained from

$$(\rho/a^2)[(a^2-u^2)u_x - uvv_x - uvu_y + (a^2-v^2)v_y] = 0, \tag{12}$$

$$-u_y + v_x = \omega, \tag{13}$$

where

$$a^2 = \frac{1}{M_\infty^2} - \frac{\gamma - 1}{2}(u^2 + v^2 - 1).$$

The jump condition (10) can be replaced by the Prandtl relation

$$q_{1n} q_{2n} = a^{*2} - \frac{\gamma - 1}{\gamma + 1} q_t^2 \tag{14}$$

and

$$q_{t_1} = q_{t_2} = q_t. \tag{15}$$

The system of equations (1)–(4) is hyperbolic in time, representing the physical unsteady process where the steady solution is reached asymptotically. Similarly, a time-dependent process can be constructed for the system (8), (9) or (12), (13). Although it does not represent a physical process, mathematically it provides a well-posed initial boundary value problem. Expanding ρ_t using the steady relation of ρ as a function of q^2 gives

$$\rho_t = -\frac{\rho}{a^2} q q_t + \rho\left(-\frac{\Delta S}{R}\right)_t. \tag{16}$$

(The last term will cancel with $\rho u(-\Delta S/R)_x + \rho v(-\Delta S/R)_y$.)

To obtain the direction of the velocity vector, the unsteady Crocco relation[17] is used:

$$\mathrm{d}\mathbf{q}/\mathrm{d}t = \mathbf{q} \times \boldsymbol{\omega} + T \nabla S. \tag{17}$$

Equation (17) gives

$$\theta_t = (-v_x + u_y) + P \frac{\mathrm{d}\,\Delta S/R}{\mathrm{d}\psi}, \tag{18}$$

where θ is the flow angle; i.e., $u = q\cos\theta, v = q\sin\theta$. Hence the magnitude of the velocity and its direction are updated using the residuals of the continuity and the vorticity equations respectively. The coefficient of equation (16) should be slightly modified to avoid problems at the stagnation points, as in Reference 11 where irrotational isentropic flows are calculated in a similar way (see also References 18 and 19).

POTENTIAL/STREAM FUNCTION FORMULATIONS

If the vorticity does not vanish identically, the potential function alone is not adequate to represent the flow field. According to the Helmholtz theorem, the velocity vector can be replaced, however, by a gradient of a scalar and a curl of another vector; hence

$$u = \phi_x + u', \tag{19}$$

$$v = \phi_y + v', \tag{20}$$

where

$$u'_x + v'_y = 0. \tag{21}$$

Equation (21) is automatically satisfied if a stream function ψ' is introduced such that

$$u' = \psi'_y, \quad v' = -\psi'_x. \tag{22}$$

With these two functions ϕ and ψ', the governing equations are:

$$(\rho\phi_x)_x + (\rho\phi_y)_y = -(\rho u')_x - (\rho v')_y, \tag{23}$$

and,
$$\psi'_{xx} + \psi'_{yy} = -\omega. \tag{24}$$

The details of such a formulation, including the boundary conditions for ψ', are given in Reference 13.

For some grids, instead of condition (21), v' can be chosen to be zero; hence $u'_y = -\omega$, which can be easily integrated to obtain u'.

Other forms are also possible; for example, instead of an additive correcion, a multiplicative factor λ is introduced such that

$$u = \lambda\phi_x, \tag{25}$$

$$v = \lambda\phi_y. \tag{26}$$

Equations (8) and (9) become

$$(\rho'\phi_x)_x + (\rho'\phi_y)_y = 0, \tag{27}$$

where $\rho' = \lambda\rho$ and

$$\phi_x\lambda_y - \phi_y\lambda_x = -\omega, \quad \frac{\partial \log\lambda}{\partial n} = -\frac{p}{\rho q^2}\frac{\partial \Delta S/R}{\partial n}, \tag{28'}$$

with $\partial n = u/q\partial_y - v/q\partial_x$. There are, however, some difficulties using this form at the stagnation point.

The general Clebsch representation[20] has both additive and multiplicative corrections and the flow field can be determined using the associated Hamiltonian system.

For two-dimensional (or axisymmetric) flows, there is no need to use two functions ϕ, ψ' or ϕ, λ. The flow field can be represented by a single stream function, for example:

$$\rho u = \psi_y, \quad \rho v = -\psi_x. \tag{29}$$

Hence, equation (8) is automatically satisfied and equation (9) becomes

$$\left(\frac{\psi_x}{\rho}\right)_x + \left(\frac{\psi_y}{\rho}\right)_y = -\omega. \tag{30}$$

The stream function formulation has other advantages. Beside the Dirichlet boundary condition on the aerofoil surface, no special treatment of the wake is needed. Also, no tracing of the streamlines is required, since at each grid point, S and ω are known in terms of ψ.

For three-dimensional flows, at least two perturbation functions ψ'_1, ψ'_2 are needed to represent the rotational perturbation part of the flow; hence, together with a potential, a total of three functions are used. On the other hand, only two stream functions are required to simulate three-dimensional flows, as shown in Reference 21.

EQUATIONS IN GENERALIZED CO-ORDINATES

If a general transformation is used,

$$\xi = \xi(x, y), \quad \eta = \eta(x, y), \tag{31}$$

the continuity and vorticity equations become

$$(\rho U/J)_\xi + (\rho V/J)_\eta = 0, \tag{32}$$

$$-\left(\frac{A_1}{J^2}V - \frac{A_2}{J^2}U\right)_\xi + \left(\frac{A_3}{J^2}U - \frac{A_2}{J^2}V\right)_\eta = -\frac{\omega}{J}. \tag{33}$$

The U and V quantities are the contravariant velocity components along the ξ and η directions respectively, A_1, A_2 and A_3 are metric quantities and J is the Jacobian of the transformation:

$$A_1 = \xi_x^2 + \xi_y^2, \quad A_2 = \xi_x \eta_x + \xi_y \eta_y, \quad A_3 = \eta_x^2 + \eta_y^2, \quad J = \xi_x \eta_y - \xi_y x_\eta.$$

Notice that

$$A_1 A_3 - A_2^2 = J^2.$$

Let

$$U = A_1 \phi_\xi + A_2 \phi_\eta + (J/\rho)\psi_\eta, \tag{34}$$

$$V = A_2 \phi_\xi + A_3 \phi_\eta - (J/\rho)\psi_\xi. \tag{35}$$

Equations (32) and (33) become

$$\left(\rho \frac{A_1}{J}\phi_\xi + \rho \frac{A_2}{J}\phi_\eta\right)_\xi + \left(\rho \frac{A_2}{J}\phi_\xi + \rho \frac{A_3}{J}\phi_\eta\right)_\eta = 0 \tag{36}$$

$$\left(\frac{A_1}{J}\frac{\psi_\xi}{\rho} + \frac{A_2}{J}\frac{\psi_\eta}{\rho}\right)_\xi + \left(\frac{A_2}{J}\frac{\psi_\xi}{\rho} + \frac{A_3}{J}\frac{\psi_\eta}{\rho}\right)_\eta = -\frac{\omega}{J}. \tag{37}$$

If $\omega = 0$, ψ can be chosen to vanish identically. On the other hand, there is no loss of generality if we choose ϕ to be zero everywhere (by applying the proper boundary condition in the far field on ψ). The speed is given by

$$q^2 = u^2 + v^2 = \frac{A_3}{J^2}u^2 - 2\frac{A_2}{J^2}uv + \frac{A_1}{J^2}v^2. \tag{38}$$

In terms of ψ only, equation (38) becomes

$$q^2 = \frac{A_3}{\rho^2}\psi_\eta^2 + 2\frac{A_2}{\rho^2}\psi_\eta\psi_\xi + \frac{A_1}{\rho^2}\psi_\xi^2. \tag{38'}$$

ψ is constant on the aerofoil; its value is determined such that the Kutta condition is satisfied at the trailing edge. For subsonic flows, a sharp trailing edge is a stagnation point. Using an 0-grid, for example, $\psi_\eta = 0$ provides the value of ψ on the body and relaxation with previous values helps the convergence. For transonic flows, the entropy on the upper surface is, in general, different from the entropy on the lower surface; the constant is chosen such that the static pressure is the same when the solution converges.

In the far field, the boundary condition is

$$\psi = y\cos\alpha - x\sin\alpha + \frac{B\Gamma}{4\pi}\ln(x^2 + B^2 y^2), \tag{39}$$

where Γ is the circulation, $B^2 = (1 - M_\infty^2)$ and α is the angle of attack. Neglecting the contribution from the vorticity generated by the shock, Γ is

$$\Gamma = \int q_b' \, ds, \tag{40}$$

where $q_b = \sqrt{A_3}\psi_h/\rho$. South[22] suggested that, if the outer boundary is located such that $x^2 + B^2 y^2$ is approximately constant, the circulation term can be subtracted from expression (39); therefore there is no need to compute the integral $\int q_b \, ds$ on the body.

It should be mentioned that a potential code can be easily modified to solve the stream function

equation. The simple iterative algorithm (assuming the density is known, solving for ψ, calculating the flux and then updating the density) converges for subsonic flows. There are some difficulties, however, in the transonic case, as discussed in Reference 23. It can be shown that a positive perturbation of the flux always produces a negative perturbation in the density according to equation (41):

$$\rho_{\text{new}} = \left[1 - \frac{\gamma - 1}{2} M_\infty^2 \left(\frac{(\rho q)^2}{\rho_{\text{old}}^2} - 1\right)\right]^{1/(\gamma-1)} e^{-\Delta S/R}. \tag{41}$$

Such an iteration may not converge in the supersonic region, since the exact relation (without freezing the density in the right-hand side) shows that a positive perturbation in the flux is associated with a positive perturbation in the density. However, if the artificial viscosity effects are dominant, and if the artificial density is under-relaxed, convergence can be obtained for some transonic cases. In general, the following algorithm is used, where U is calculated from

$$-\left[\left(\frac{A_1}{J^2}\theta - \frac{A_2}{J^2}\right)U\right]_\xi + \left[\left(\frac{A_3}{J^2} - \frac{A_2}{J^2}\theta\right)U\right]_\eta = -\frac{\omega}{J}, \tag{42}$$

where $\theta = -\psi_\xi/\psi_\eta$. Equation (42) is solved along constant ξ lines marching towards the body in two boxes, including the supersonic regions. Once U is known, V is calculated from the relation $V = \theta U$. Then the density is updated in terms of V and U. A compact scheme for discretizing equation (42), consistent with the calculations of the residual in terms of ψ (equation (37)), produces sharp shocks where no excessive artificial viscosity and no under-relaxation of the density are required.

For complex geometries, the body-fitted co-ordinates are not simple to construct. Cartesian co-ordinates (with exact boundary conditions) have been used successfully in Reference 24 for subsonic flows. Adopting the present formulation, transonic flows can be calculated in a similar way (atleast for engineering purposes). In this respect, the Dirichlet boundary condition is easier than the corresponding Neumann condition for the potential equation, which has also been successfully solved on Cartesian co-ordinates in Reference 25.

APPROXIMATE MODELS

The alternative formulations, described above, are equivalent to Euler equations. Whether a system of first-order equations in u and v (q and θ), a potential function plus some correction or a stream function is used, shocks must be detected to calculate the entropy jumps. The momentum equations are satisfied through requiring that the entropy and the vorticity over the pressure, ω/p, are constants along streamlines downstream of a shock. Certain approximations lead to simplified models; their usefulness, however, depends on the validity of the assumptions made. In the following, four such models are examined.

I. Irrotational isentropic flow

It is assumed that both S and ω are negligible. The x and y momentum equations are replaced by the conditions $\omega = 0$ and $S = 0$. The continuity equation in conservation form and the irrotationality condition can be solved simultaneously without any shock identification procedure. The irrotationality condition can be automatically satisfied if a potential is used, while a stream function satisfies the continuity equation by construction. The second-order equation of the potential or the stream function has the same characteristics and it can be shown that the potential lines are perpendicular to the streamlines.

The mass and the energy are conserved but the momentum is not. The drag can be calculated in terms of the normal momentum losses across shocks:

$$D = \int_{\text{shocks}} \sin\beta(\rho q_n^2 + p)\,\mathrm{d}l, \tag{43}$$

where β is the angle of the shock relative to the free stream direction. For a one-dimensional flow, expanding ρ and p in terms of u, where $u = 1 + \bar{u}$, the jump in momentum, assuming mass is conserved, is given by

$$\rho(1+\bar{u})\bar{u} + \Delta p = \frac{M_\infty^2(\gamma+1)\bar{u}^3}{12}\left(1 + (1 - M_\infty^2)\frac{2-\gamma}{1+\gamma}\right). \tag{44}$$

The first term in expression (44) is an approximation of the entropy which would have been produced if the isentropic condition were relaxed.

Across the wake, the pressure, density and tangential velocity are continuous; the circulation is determined such that the static pressure at the trailing edge is the same on the upper and the lower surfaces.

II. Irrotational non-isentropic flows

The entropy jump in equation (5) depends on the Mach number upstream of the shock and the shock inclination; the vorticity, however (equation (6)), depends on the shock curvature. (Downstream of a straight shock, the vorticity vanishes; i.e., the flow remains irrotational but with a different level of entropy.) Assume the shock curvature is neglected, $\omega = 0$, but $\Delta S \neq 0$; in this model, the mass, energy and momentum in the streamwise direction are conserved. The momentum normal to streamlines is not conserved, however, due to the present approximation. The mass balance across a shock is given by

$$(\rho q_n)_1 = (\rho q_n)_2 = (\rho_i \mathrm{e}^{-\Delta S/R} q_n)_2. \tag{45}$$

The corresponding relation in the isentropic irrotational approximation does not include the factor $\mathrm{e}^{-\Delta S/R}$; i.e., the difference between the two models is approximately a source distribution along the shock, where the strength of such a source depends on the entropy jump. Notice that the changes of the velocity field, Δq, due to the entropy term is not small:

$$\frac{\Delta q}{q} = \frac{\Delta S/R}{1 - M^2}.$$

At the foot of the shock, there is a singularity, since there will be in general a mismatch between the curvature of the streamlines satisfying the shock jump conditions and the wall curvature. It is assumed that the vorticity there is finite.

Since $\Delta S/R = f(M_0^2)$, where $M^2 = M^2 \sin^2\beta$, the derivative with respect to ψ is

$$\frac{\mathrm{d}\,\Delta S/R}{\mathrm{d}\psi} = \frac{\partial f}{\partial M_n^2}\left(\sin^2\beta\frac{\partial M^2}{\partial \psi} + 2M^2 \sin\beta\cos\beta\frac{\mathrm{d}\beta}{\partial\psi}\right). \tag{46}$$

It is required that $\cos\beta\,\mathrm{d}\beta/\mathrm{d}\psi$ be bounded. This is true in the Zierep–Oswatitsch theory[26] where $(\xi/\eta)_{\text{shock}} = \eta \ln\eta$ (ξ is tangential to the wall and η is tangential to the shock at the singular point). It is also true in other theories; for example, if $\xi = \eta^{3/2}$. Based on the numerical solution of Euler equations, it seems that the singularity has the same form as in the potential calculations or, in other words, the vorticity effects can be neglected there, as will be discussed later. Since the pressure

far downstream, P_d, is not uniform due to the entropy variation, the drag based on a control volume enclosing the aerofoil is

$$D = \int_A (P_\infty - P_d)\,dA = P_\infty \int_A (\Delta S/R)\,dA. \tag{47}$$

Across the wake, the density jumps due to the different levels of entropy. If the pressure is made continuous, there will be a circulation generated along the wake due to a jump in the tangential velocity. At a sharp trailing edge, if the pressure is forced to be the same on the upper and lower surfaces, the flow will leave tangential to the surface of lower entropy.

A modified potential formulation. Since the flow is assumed to be irrotational, a single potential function can be used (i.e., there is no rotational correction and ψ' vanishes everywhere since $\omega = 0$). The density has to be modified by the entropy function and hence it appears that the entropy has to be known everywhere downstream of the shock. Some simplification can be achieved; namely, expanding the continuity equation gives

$$e^{-\Delta S/R}[(\rho_i\phi_x)_x + (\rho_i\phi_y)_y] + \rho_i\phi_x(e^{-\Delta S/R})_x + \rho_i\phi_y(e^{-\Delta S/R})_y = 0. \tag{48}$$

The last two terms cancel and equation (48) reduces to the classical potential equation, except across shocks and wakes where the entropy jumps. Since the body is a streamline, no special treatment is required there. No special grids are needed as in Reference 15 and extension to three-dimensions* is straight forward. A variational formulation is given in Reference 28.

To calculate the pressure, it is noticed that the formula ρ_i^γ may be closer to Euler results than $\rho_i^\gamma e^{-\Delta S/R}$ (except at the trailing edge). If the correction due to the vortcity is u' (where v' is set equal to zero), equation (9) becomes

$$u'_y \simeq -\frac{P}{\rho q}\frac{\partial \Delta S/R}{\partial y} \tag{49}$$

or

$$u' \simeq -\frac{P}{\rho q}\Delta S/R. \tag{50}$$

Expanding the formula for the pressure including the vorticity effects, gives

$$p = (p_i + \delta p)e^{-\Delta S/R} \simeq p_i - \rho q u' - \Delta S/R\, p_i. \tag{51}$$

Using equation (50), the last two terms in equation (51) cancel each other and thus the pressure is given by the isentropic formula in terms of the irrotational speed. Hence, across the wake, assuming the isentropic pressure to be continuous is a good approximation except near the trailing edge.

Computational algorithms. To implement the modified potential formulation, a shock point operator is introduced to satisfy equation (45). First, a comparison with Murman's scheme for the small-disturbance equation is given. In the non-conservative scheme of Murman and Cole, central differences are used across the shock. For example, if the shock is located between the grid points i and $i-1$, the flux term $(\phi_x^2)_x$ is discretized using ϕ_i and ϕ_{i-1}, while $(\phi_x^2)_x$ is discretized using ϕ_i, ϕ_{i-1} and ϕ_{i+1}:

* For an unyawed elliptic wing with a self-similar wing section (where the loading is elliptic and Prandtl lifting-line theory gives good results[29]), the isentropic potential solution may not be unique and there is a need for such a non-isentropic formulation.

$$(\phi_x^2)_x \simeq 2\phi_x\phi_{xx} = 2\frac{\phi_{i+1}-\phi_{i-1}}{2\Delta x}\frac{\phi_{i+1}-2\phi_i+\phi_{i-1}}{\Delta x^2}. \tag{52}$$

The corresponding conservative operator is given in terms of $\phi_i, \phi_{i+1}, \phi_{i-1}$ and ϕ_{i-2}, where differences across shocks are avoided:

$$(\phi_x^2)_x = \frac{1}{\Delta x}\left[\left(\frac{\phi_{i+1}-\phi_i}{\Delta x}\right)^2 - \left(\frac{\phi_{i-1}-\phi_{i-2}}{\Delta x}\right)^2\right]. \tag{53}$$

Equation (53) can be rewritten as the sum of central difference and backward difference operators. It can be shown that using equation (53) is the same as fitting a normal shock between i and $i-1$ points.[30] Lock[5] suggested using a weighted average of the two operators; namely,

$$(\phi_x^2)_x = (1-\lambda)\frac{\phi_{i+1}-\phi_{i-1}}{\Delta x}\frac{\phi_{i+1}-2\phi_i+\phi_{i-1}}{\Delta x^2} + \lambda\frac{\phi_i-\phi_{i-2}}{\Delta x}\frac{\phi_i-2\phi_{i-1}+\phi_{i-2}}{\Delta x^2}. \tag{54}$$

λ is chosen (empirically) to satisfy the Rankine–Hugoniot relations across the shock. To fix the factor λ, Prandtl's relation is suggested in Reference 31. In Reference 32, the following form is used:

$$\left(1+\frac{\phi_{i+1}-\phi_i}{\Delta x}\right)\left(1+\frac{\phi_{i-1}-\phi_{i-2}}{\Delta x}\right) = a^{*2}. \tag{55}$$

For the full potential equation in conservation form, equation (55) is replaced by

$$\rho_{i-3/2}u_{i-3/2} = \rho_{i+1/2}u_{i+1/2}e^{-\Delta S/R}, \tag{56}$$

where

$$\Delta S/R = f(M^2_{i-3/2}). \tag{57}$$

The four operators (52)–(56) are summarized in Table I.

III. Rotational isentropic flows

In this model, the mass and the momentum are conserved. The flow is forced to be isentropic ($S=0$), hence the energy is not conserved. Thus there is, in general, a vorticity generated by the shock and $\omega \neq 0$. So if equations (1)–(3) are solved and equation (4) is replaced by the isentropic relation for the pressure, h is not constant downstream of the shock and the vorticity is (Δh is a function of ψ only)

$$\omega = -\rho \mathrm{d}\,\Delta h/\mathrm{d}\psi. \tag{58}$$

Table I. Comparison of shock operators

	f^{--} f^{-} f^{+} i − 2 i − 1 Shock i i + 1
Murman's conservative operator:	$f^+ - f^{--} = 0$
Murman's non-conservative operator:	$f^+ - f^{--} = (f^- - f^{--})$
Lock's scheme:	$f^+ - f^{--} = (1-\lambda)(f^- - f^{--})$
Present scheme:	$f^+ - f^{--} = (\Delta S/R)(f^+ + 1)$

Table II. Comparison of approximate models

Model	x–m	y–m	Energy	Mass	Entropy	Vorticity
I	NC	NC	C	C	C	C
II	C	NC	C	C	NC	C
III	C	C	NC	C	C	NC
IV	C	C	C	NC	C	NC
Euler	C	C	C	C	NC	NC

C = conserved. NC = not conserved.

Based on energy losses, the drag is

$$D = -\frac{1}{q_\infty} \int_{\text{shocks}} \rho q_n \Delta h \, dl. \tag{59}$$

This model has been used by Magnus and Yoshihara[1] to calculate transonic flows. It is interesting to notice that the differences between the quantities downstream of a shock in this model and in Euler calculations are small.

IV. Isoenergetic isentropic flows

Viviand[11] suggested solving the momentum and energy equations together with the isentropic relation. The density is updated in terms of the flux as in the stream function formulation. Mass is not conserved and the drag can be estimated in terms of the mass unbalance across shocks.

The conservative quantities of the four models are summarized in Table II. The shock polars for some of these models are given by Viviand.[11] The special case of a normal shock (one-dimensional flow) is also studied in Reference 15. It should be mentioned that the non-isentropic irrotational case has the same shock polar as the Euler equations and fitting Rankine–Hugoniot shocks in potential calculations yields comparable results to Euler solutions.

NON-UNIQUENESS PROBLEMS

There is no proof that the steady Euler equations have a unique solution in the transonic regime. There are some questions, however, whether certain approximations (e.g., isentropic assumption) are responsible for some non-uniqueness problems. The quasi-one-dimensional flow in a convergent–divergent nozzle is a simple and interesting problem. If potential formulation is used, non-unique solutions are possible. Excluding expansion shocks for physical reasons, the position of a compression shock is not uniquely determined. Even if the shock strength is fixed, there are three possibilities when the inlet condition is supersonic: (i) a shock in the divergent part; (ii) a shock in the convergent part; (iii) two shocks, one in the convergent part of the nozzle and the other in the divergent part. Similarly, Euler equations have non-unique solutions, but some of the non-unique solutions of the potential equation are not admissible as Euler solutions. If the back pressure is prescribed, the potential solution may not exist, while non-unique Euler solutions with the same entropy can be constructed. If artificial viscosity (satisfying entropy inequality) is added to Euler equations, expansion shocks are eliminated but non-unique solutions of compression shocks are still possible. It is known, however, that shocks in the convergent part of the nozzle are physically unstable;[33], hence, if a time-dependent marching scheme representing the physical unsteady

process is used, such a solution will be automatically excluded. On the other hand, with Newton's method, the unstable solution may be obtained numerically.

The problems of two-dimensional flows are more complicated. Consider the small-disturbance equation with uniform viscosity:[34]

$$v\psi_{xxx} - \phi_x\phi_{xx} + \phi_{yy} = 0. \tag{60}$$

Assuming there are two solutions ϕ_1 and ϕ_2 satisfying equation (60) and the boundary conditions (say, flow in a channel where ϕ and ϕ_x are given at the inlet, ϕ is given at the exit, $\phi_y = f'(x)$ at the wall $y = f(x)$ and at the axis of symmetry $\phi_y = 0$), the equation for the difference between the two solutions, $\varepsilon = \phi_1 - \phi_2$, is

$$v\varepsilon_{xxx} - \tfrac{1}{2}(\phi_{1x}^2 - \phi_{2x}^2) + \varepsilon_{yy} = 0. \tag{61}$$

Multiplying equation (55) by ε and integrating by parts gives

$$\iint \tfrac{1}{2}\varepsilon_x^2(u_1 + u_2) - \varepsilon_y^2 \,\mathrm{d}x\,\mathrm{d}y - \int_{\text{axis + wall}} \varepsilon\varepsilon_y \,\mathrm{d}y$$

$$+ \int_{\text{exit + inlet}} v\varepsilon\varepsilon_{xx} - \tfrac{1}{2}v\varepsilon_x^2 - \tfrac{1}{2}\varepsilon\varepsilon_x(u_1 + u_2)\,\mathrm{d}y = 0. \tag{62}$$

The only boundary term which does not necessarily vanish is

$$-\tfrac{1}{2}v\int_{\text{exit}} \varepsilon_x^2 \,\mathrm{d}y.$$

It is clear that if $u_1 + u_2$ is negative (subsonic flows), ε should be identically zero; therefore the solution is unique. In general, the viscosity term drops out except at the boundary and the non-uniqueness problem is not settled for transonic flows. Even if artificial viscosity and time-dependent marching schemes are used, a steady unique solution cannot be guaranteed.

It is noticed, however, that in the existing potential codes, the artificial viscosity is switched off in the subsonic region to produce sharp shocks. In Euler codes, viscosity is used everywhere for stability reasons. Some numerical experiments with uniform viscosity in potential codes indicate that the problem of non-uniqueness can be, at least, postponed. Shocks, of course, are more smeared, but the solutions are still meaningful. Two forms of artificial densities are tested in the present work:

$$\bar{\rho} = \rho - \mu\rho_s\Delta s \tag{63}$$

and

$$\bar{\rho} = \rho + \mu q_s\Delta s, \tag{64}$$

where μ is a constant in the shock region. Equation (64) produces an artificial viscosity term of the form $\mu[(uq_s)_x + (vq_s)_y]$ which is an approximation of $\mu\phi_{sss}$. In Reference 35, a variable continuous μ is suggested and it is claimed that only dissipative terms are thus produced; it is not clear, however, how the lower-order terms (because of the conservation form) are cancelled.

If a second-order form of shifting density, velocity or flux is used, the resulting scheme is not dissipative; for example,

$$\bar{\rho} = \rho - \mu(\rho_i - \rho_{i-1}) - \varepsilon(\rho_{i-1} - \rho_{i-2}). \tag{65}$$

ε can be chosen, however, such that equation (65) reduces to a first-order (dissipative) formula in the shock region.

In passing, sharp shocks are obtained in Reference 6 as a limit of a sequence of calculations using equation (63).

It should be mentioned that the solution is dependent on the amount of the artificial viscosity introduced through the discretization process. Moreover, by refining the mesh, more artificial viscosity may be needed and the numerical solution does not approach the exact solution of the inviscid partial differential equation.

Instead, the potential differential equation may be replaced by the viscous transonic equation where the coefficient of the viscous term can be determined in terms of Prandtl and Reynolds numbers (Reference 34). Assuming that the viscous transonic differential equation has a unique solution, it may be possible to construct a discrete analogue which also has a unique solution.

NUMERICAL RESULTS

Three sets of results are presented (Figures 1–11). First, the stream function results, where $s = 0$ and $\omega = 0$, are compared with Euler solutions. Second, the modified potential results, $s \neq 0$ and $\omega = 0$, are shown, together with the potential calculations with uniform viscosity in the shock region. Third, the results of the isentropic rotational formulation (where mass and momentum equations are solved for isentropic flows) are given.

All these results are obtained using the CDC 203 computer. The Euler solutions are produced from Flo 52-S,[37] a modified version of Jameson's Runge–Kutta finite volume code.* The potential solutions are calculated using Zebra relaxation.[38] The stream function solutions are obtained by modifying the potential code.

All the calculations are for a NACA 0012 aerofoil. An 0-grid of 120 × 34 points is used for the

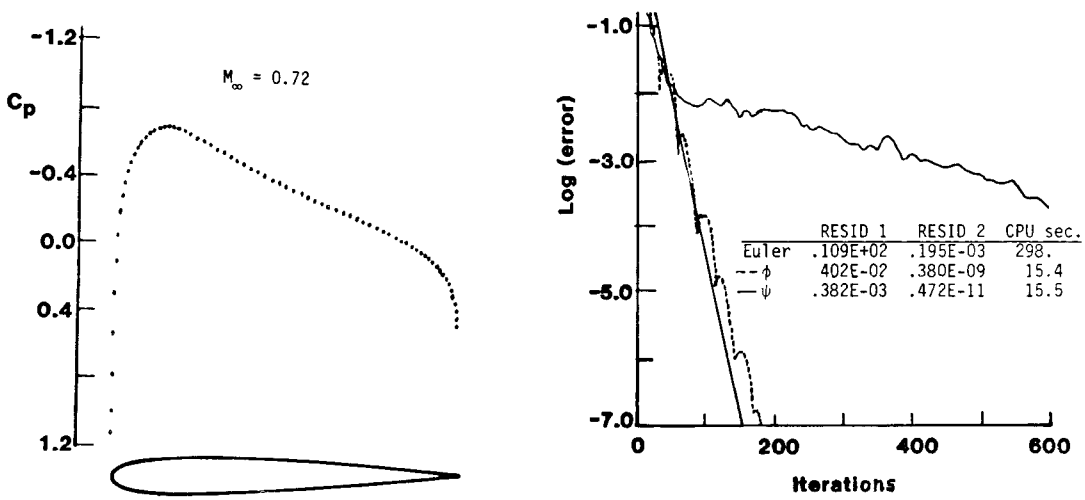

(a) (b)

Figure 1. Potential, stream function and Euler solutions for a subsonic case

* Recently, Jameson[39] successfully applied multigrid techniques to Euler calculations where very fast convergence to steady state solutions is achieved. The same acceleration techniques are equally applicable, however, to both potential and stream function calculations.

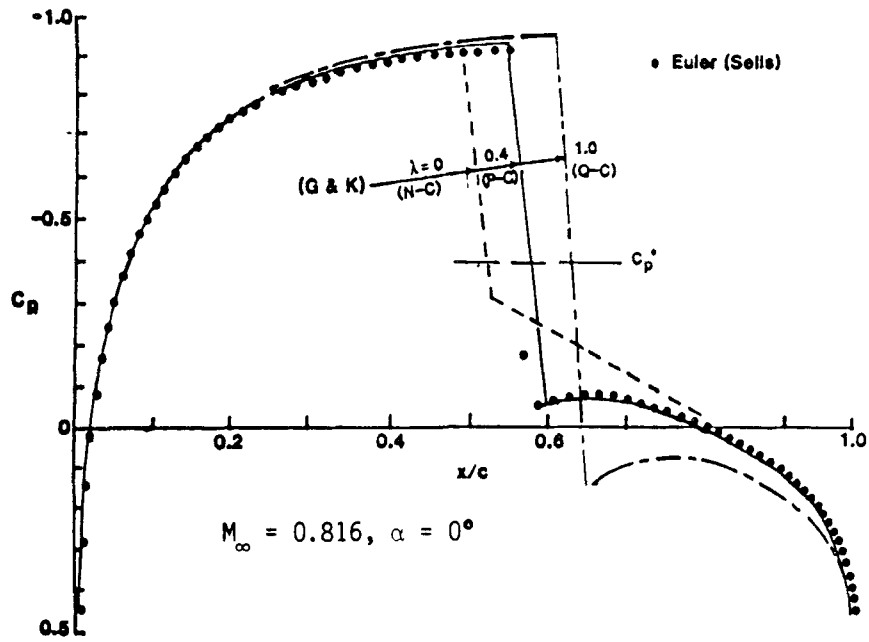

(a)

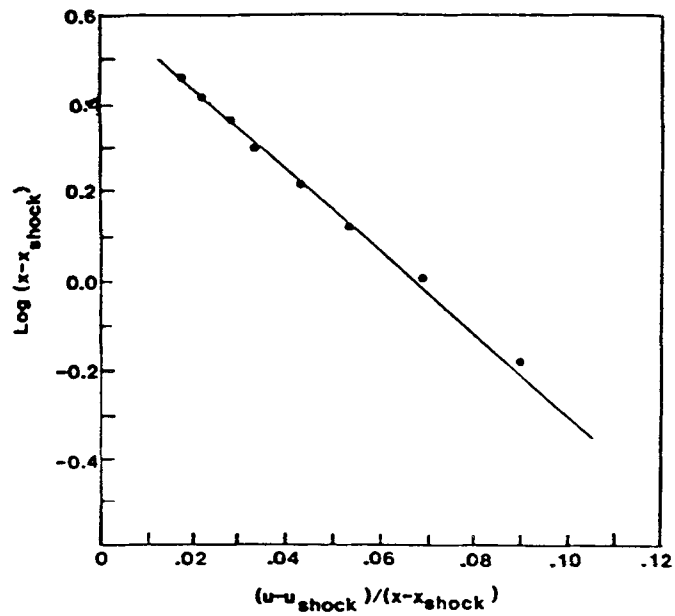

(b)

Figure 2. (*a*) Comparison between Lock's result and the Euler solution (after Sells). (*b*) The behaviour of the Euler solution at the foot of the shock

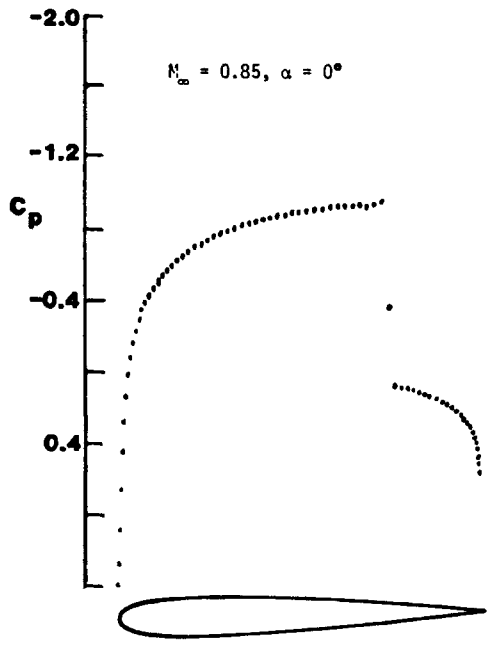

(a)

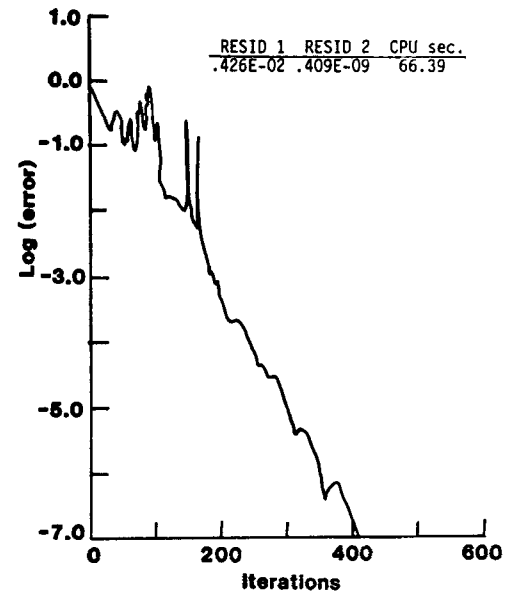

(b)

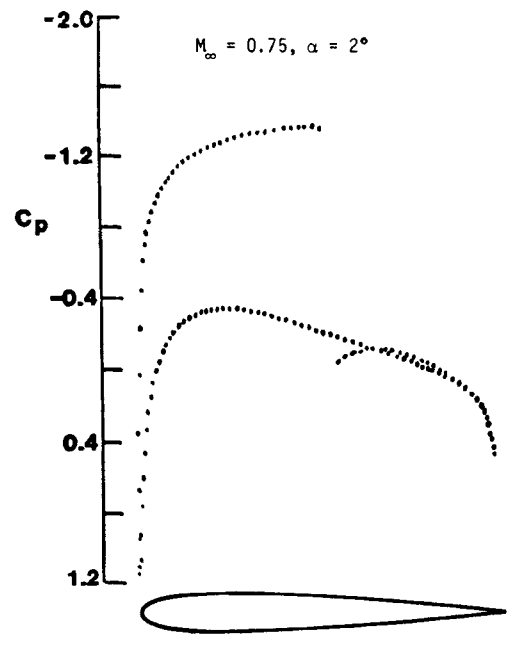

(c)

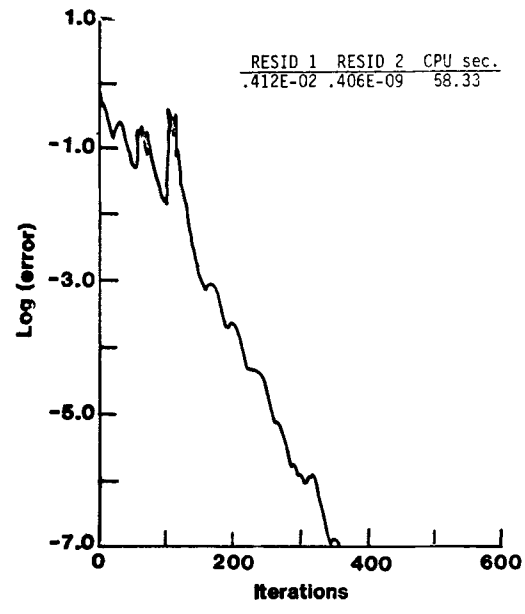

(d)

Figure 3. Modified potential solutions, including entropy corrections

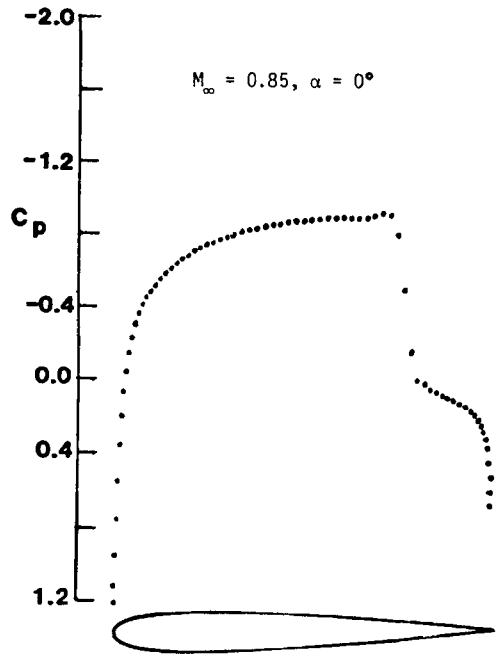

(a)

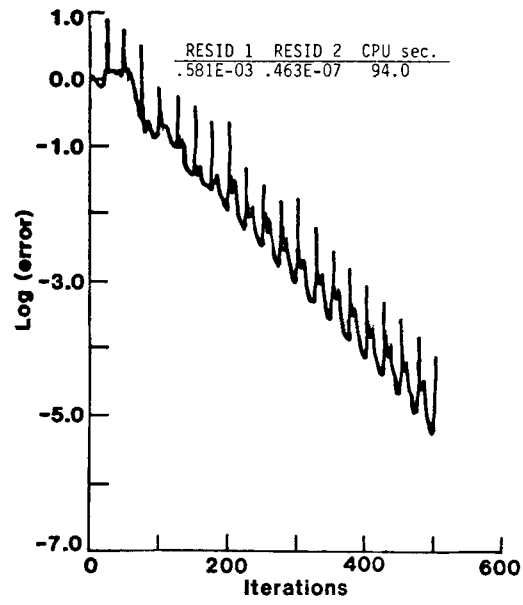

(b)

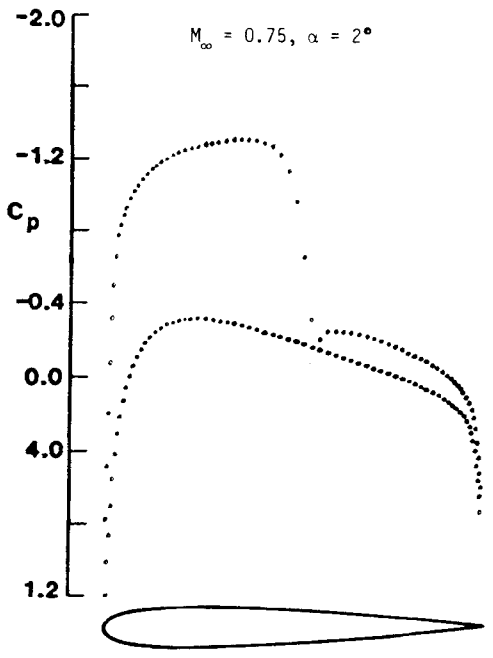

(c)

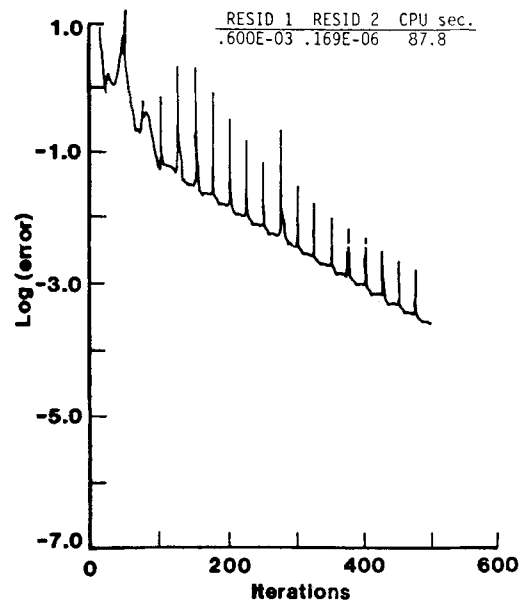

(d)

Figure 4. Stream function solutions ($S \neq 0$, $\omega = 0$)

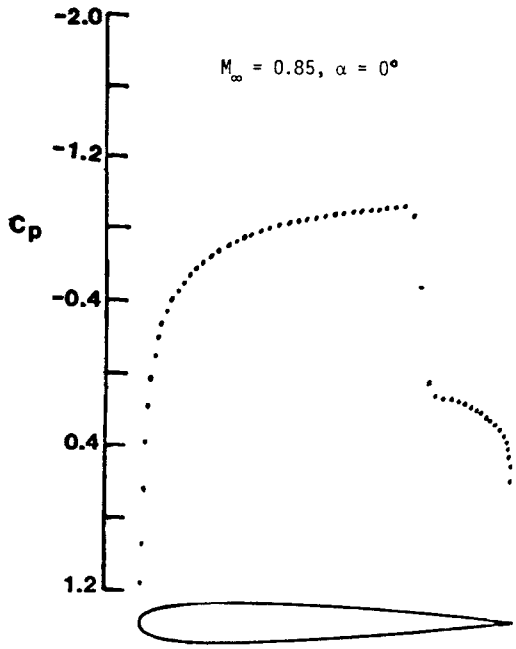

(a)

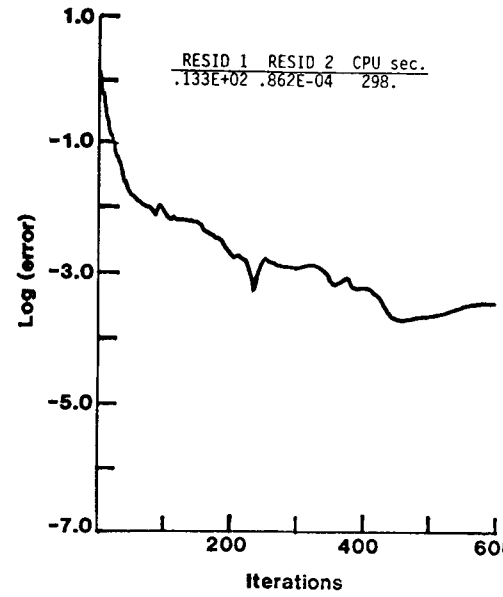

(b)

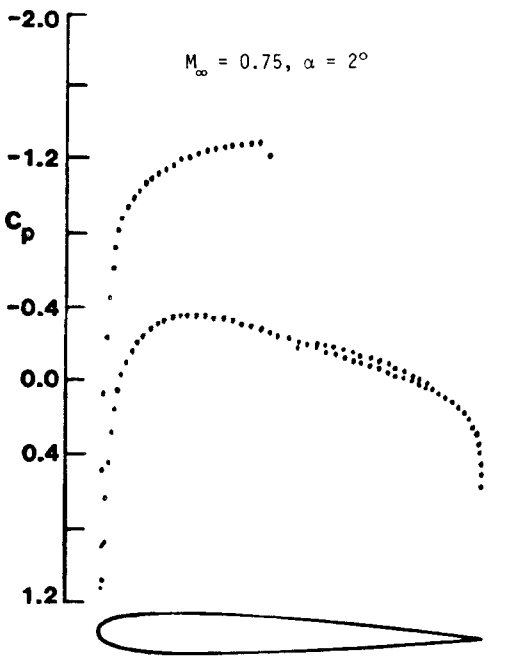

(c)

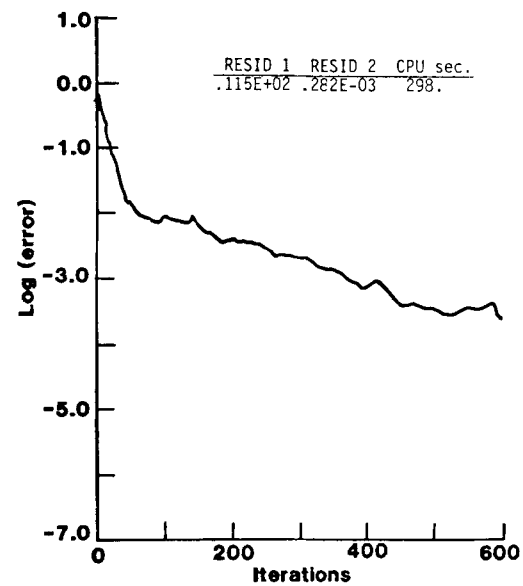

(d)

Figure 5. Euler solutions

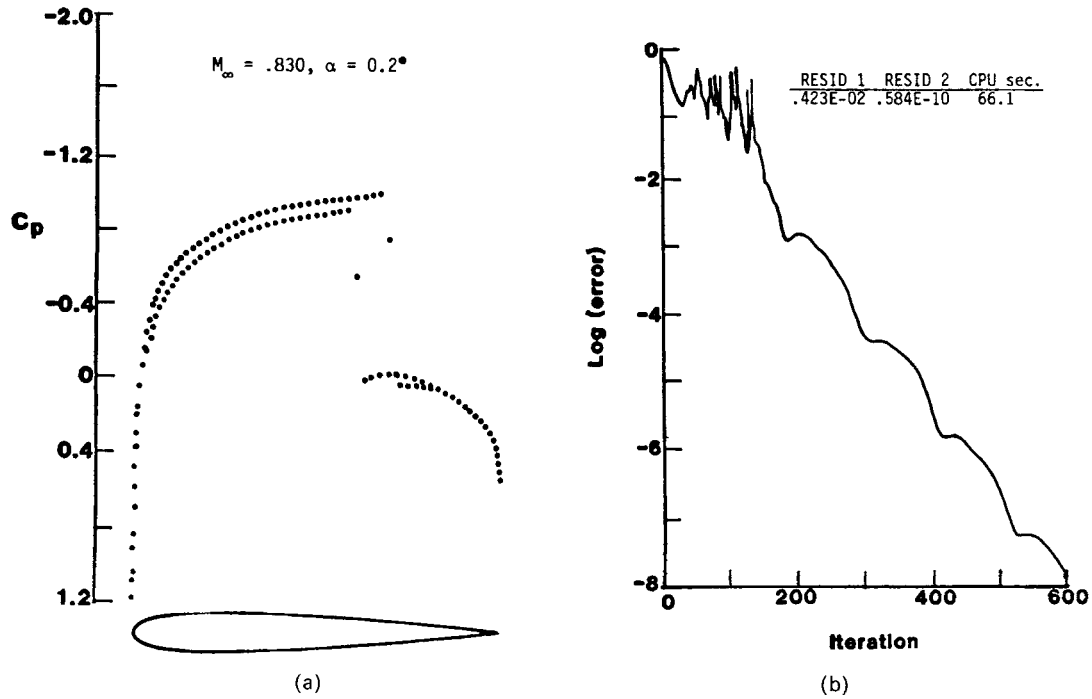

Figure 6. Modified potential solution, including entropy correction, in the non-uniqueness range

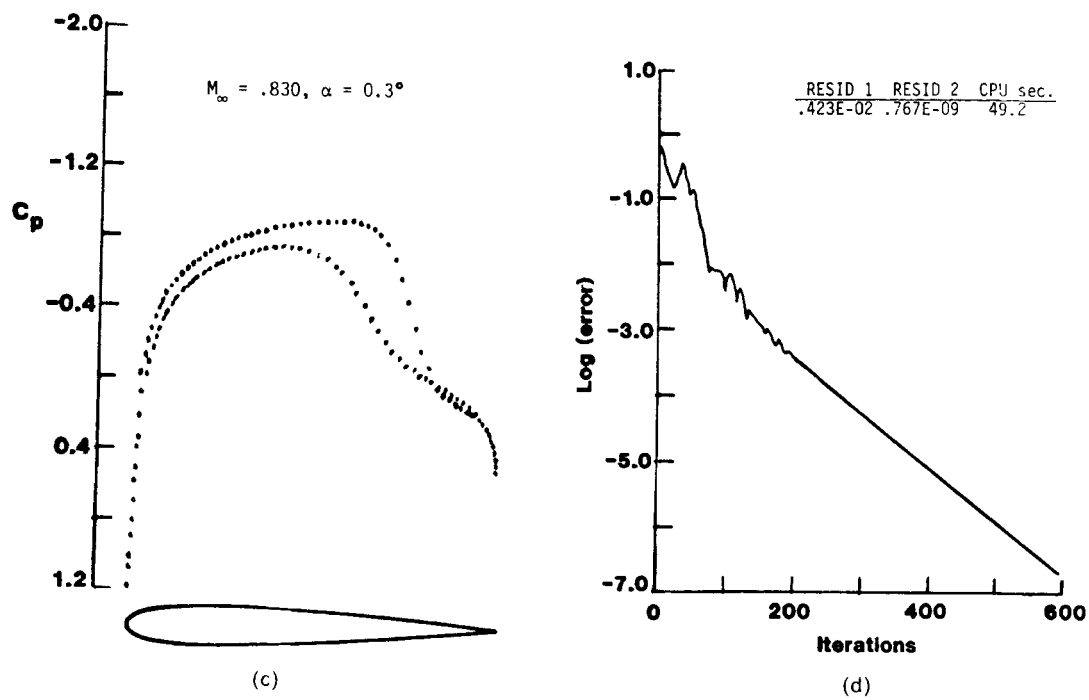

Figure 7. Potential solution, with uniform artificial viscosity in the shock region, in the non-uniqueness range

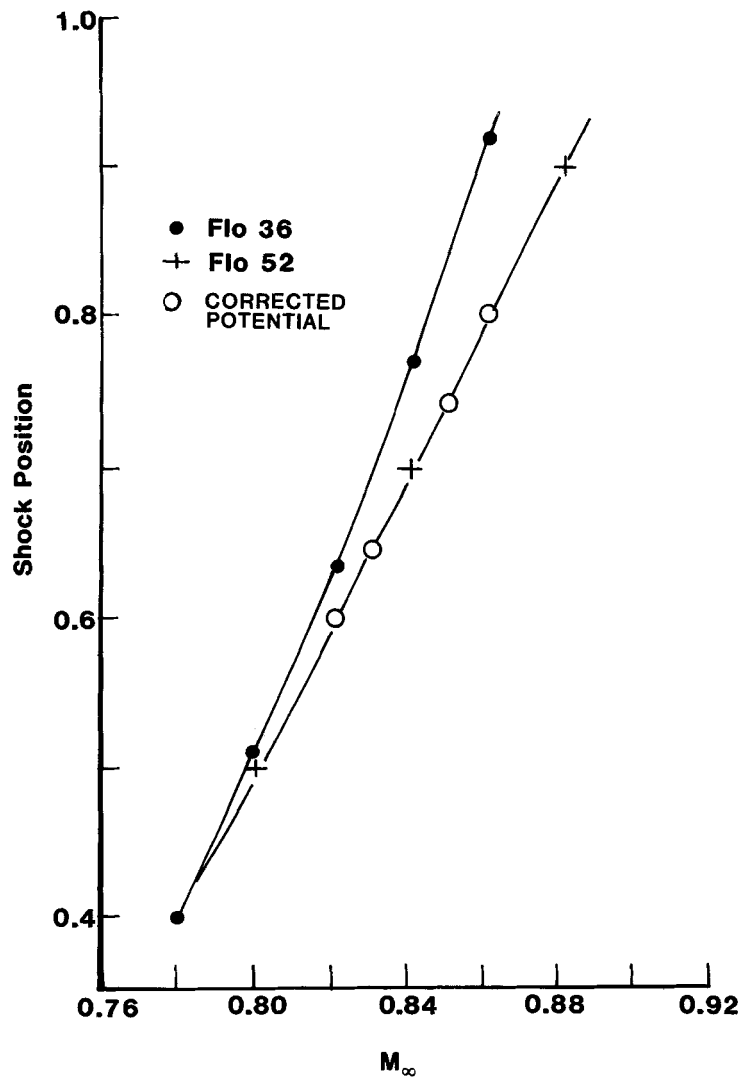

Figure 8. Shock position versus Mach number for non-lifting flows

Euler calculations. The grid of the potential and stream function is slightly different (149 × 30).

The pressure distributions on the surface of the aerofoil and the convergence histories (maximum residuals versus number of iterations) are plotted for different Mach numbers and angles of attack. Euler calculations are, of course, more expensive than potential or stream function ones. They are 20–5 times slower (in terms of CPU seconds) depending on the Mach number. C_l–α curves for $M_\infty = 0{\cdot}83$ and $0{\cdot}79$ are given for different models. The drag and the shock position variations with Mach numbers at zero angle of attack are also shown. A comparison between the Euler solution and Lock's result using his quasi-conservative scheme is given after Sells.[10] At the foot of the shock, the Euler solution behaves as in the potential calculations;[30] namely, $(u - u_{\text{shock}})$ is proportional to $(x - s_{\text{shock}}) \log (x - x_{\text{shock}})$. The vorticity effects are indeed small and can be neglected, especially for the symmetric cases at zero angle of attack. For a lifting aerofoil, the flow is forced to have a stagnation point at the trailing edge, as in the potential calculation, and the streamline leaving the aerofoil bisects the trailing edge angle. This aspect is a subject of further investigation.

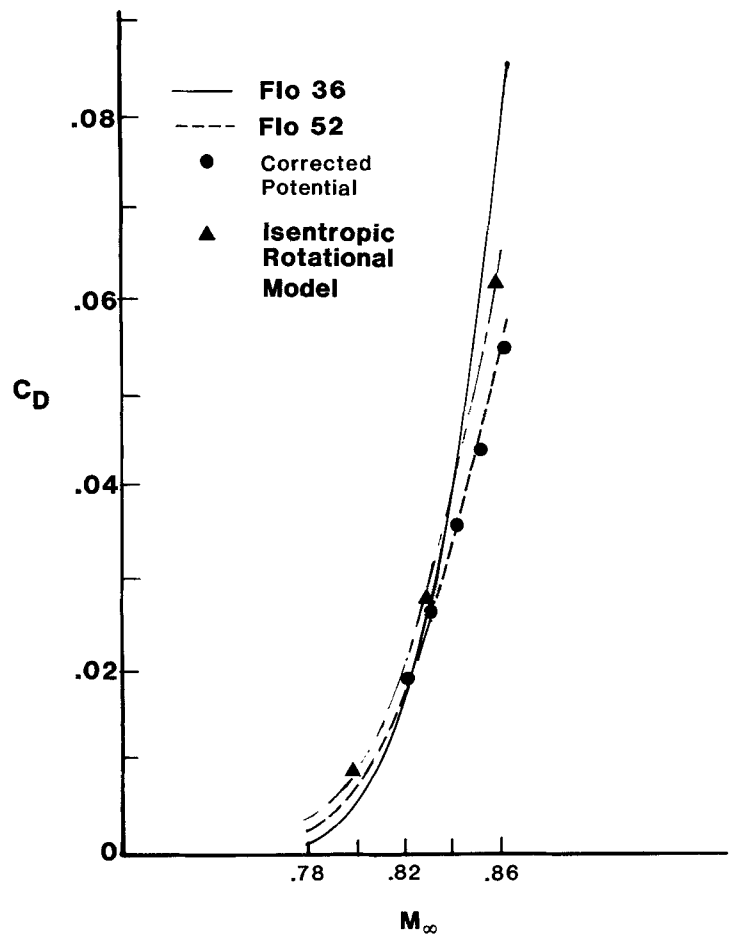

Figure 9. Drag versus Mach number for non-lifting flows

CONCLUDING REMARKS

First, it is shown that isentropic irrotational transonic flows can be calculated using the stream function, in a body-fitted co-ordinate system, in the same way a potential equation is solved.

If entropy effects are included in potential or stream function formulations, closer results to the Euler solution are obtained; particularly in the range where existing codes (without entropy modifications) produce non-unique solutions.

However, non-uniqueness is not only due to the isentropic assumption. For example, if mass and momentum equations together with the isentropic relation ($p \alpha \rho^{\gamma}$) are solved, unique solutions are obtained in the same range where the isentropic potential solution is not unique.

Unique solutions are also obtained with existing potential codes if enough uniform artificial viscosity in the shock region is used, but shocks are smeared. Thus, by weakening the shock due to entropy, vorticity or artificial viscosity effects, the non-uniqueness problem is avoided for the cases considered.

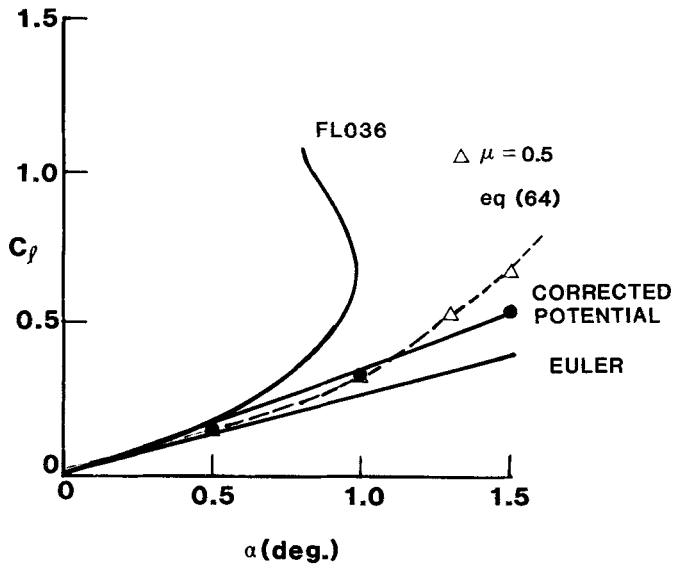

Figure 10. Lift versus angle of attact for $M_\infty = 0.79$

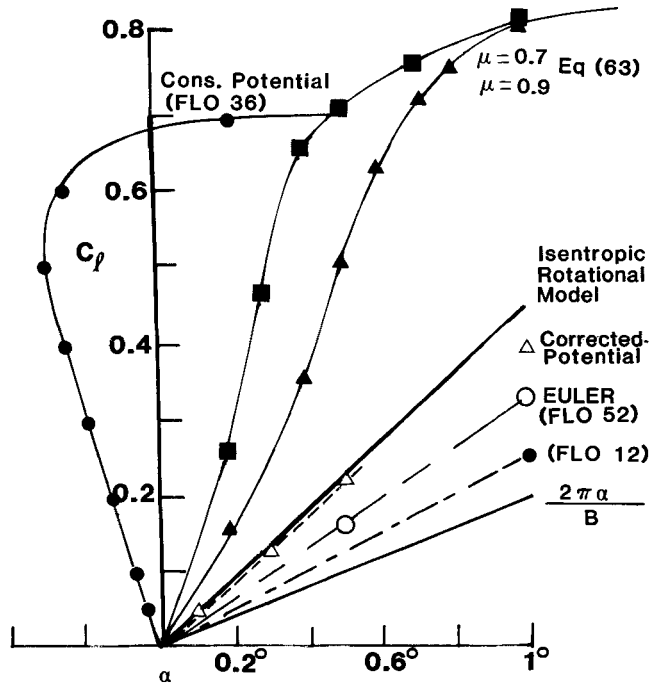

Figure 11. Lift versus angle of attack for $M_\infty = 0{\cdot}85$

ACKNOWLEDGEMENTS

This work is supported by the NASA Langley Research Center. The authors would like to thank Jerry South and Many Salas for many helpful discussions.

REFERENCES

1. R. Magnus and H. Yoshihara, 'Inviscid transonic flow over airfoils', *AIAA J.*, **8,** 2157–2161 (1970).
2. E. M. Murman and J. D. Cole, 'Calculation of plane steady transonic flow, *AIAA J.*, **9,** 114–121 (1971).
3. E. M. Murman, 'Analysis of embedded shock calculated by relaxation methods', *AIAA J.*, **12,** 626–633 (1974).
4. A. Jameson, 'Transonic flow calculations', *VKI Lecture Series, Vol. 87*, March 1976.
5. M. R. Collyer and R. C. Lock, 'Improvements to the viscous Garabedian and Korn method for calculating transonic flow past an airfoil', *RAE Technical Report 78039*, 1978.
6. J. Steinhoff and A. Jameson, 'Multiple solutions of the transonic potential flow equation', *AIAA J.*, **20,** 1521–1525 (1982).
7. M. Salas, A. Jameson and K. Melnik, 'A comparative study of the nonuniqueness problem of the potential equation', *AIAA Paper 83-1888-CP*, 1983.
8. J. L. Steger, 'Implicit finite difference simulation of flow about arbitrary two-dimensional geometries', *J. Comput. Phys.*, **16,** 679–686 (1978).
9. A. Lerat, 'Implicit methods of second-order accuracy for the Euler equations', *AIAA Paper 83-1925-CP*, 1983.
10. C. C. Sells, 'Solution of the Euler equations for transonic flow past a lifting aerofoil', *RAE Technical Report 80065*, May 1980.
11. H. Viviand, 'Pseudo unsteady methods for transonic flow computations', *Proc. Seventh Int. Conf. on Numerical Methods in Fluid Dynamics*, Stanford, 1980, Springer, 1981.
12. A. Jameson, W. Schmidt and E. Turkel, 'Numerical solutions of the Euler equations by finite volume methods using Runge–Kutta time-stepping schemes', *AIAA Paper 81-2159*, 1981.
13. M. Hafez and D. Lovell, 'Transonic small disturbance calculations including entropy corrections', *Symp. on Numerical and Physical Aspects of Aerodynamics Flows*, California State University, Long Beach, January 1981.
14. L. T. Chen, Transonic flowfield computation using a modified shock-point operator', *Second Symp. on Numerical and Physical Aspects of Aerodynamic Flows*, California State University, Long Beach, January, 1983.
15. G. H. Klopfer and D. Nixon, 'Non-isentropic potential formulation for transonic flows', *AIAA Paper 83-0375*, 1983.
16. J. Steger, and B. Baldwin, 'Shock waves and drag in the numerical calculation of isentropic transonic flow', *NASA TN D-6997*, October 1972.
17. H. Liepman and A. Roshko, *Elements of Gas Dynamics*, Wiley, 1957.
18. C. Welford and M. Hafez, 'Implicit velocity formulation for the calculation of transonic flow by finite element method', *Comput. Methods Appl. Mech. Eng.*, **22,** 161–186 (1980).
19. S. Osher, M. Hafez and W. Whitlow, 'Entropy condition satisfying approximations for the full potential equation of transonic flow', *Math. Comput.* (January 1985).
20. A. Ecer and H. U. Akay, 'A finite element formulation for steady transonic Euler equations', *AIAA J.*, **21,** 343–350 (1983).
21. A. Sherif and M. Hafez, 'Computation of three-dimensional flows using two-stream functions', *AIAA Paper 83-1948-CP*, 1983.
22. J. South, Private communication.
23. M. Hafez and D. Lovell, 'Numerical solution of transonic stream function equation', *AIAA J.*, **21,** 327–335 (1983).
24. R. Noack and D. Notron, 'Two-dimensional, subsonic, flowfield analysis for arbitrary boundaries with lifting bodies', *AIAA Paper 82-0221*, 1982.
25. B. Wedan and J. South, 'A method for solving the transonic full potential equation for general configurations', *AIAA Paper 83-1889-CP*, 1983.
26. H. Oswatitsch and J. Zierep, 'Das Problem des Senkrechten Strossen an Einer Gekrummten Wand', *ZAMM*, **40** (Suppl.), 143–144 (1960).
27. C. Ferrari and F. Tricomi, *Transonic Aerodynamics*, Academic Press, New York, 1968.
28. M. Hafez, 'Progress in finite element techniques for transonic flows', *AIAA Paper 83-1919-CP*, 1983.
29. M. Hafez, 'Perturbation of transonic flow with shocks', in T. Cebeci (ed.), *Proc. Symp. on Numerical and Physical Aspects of Aerodynamic Flows*, Springer, 1982.
30. M. Hafez and H. K. Cheng, 'Shock fitting applied to relaxation solutions of transonic small-disturbance equations', *AIAA J.*, **15,** 786–793 (1977).
31. M. Hafez and E. Murman, 'A shock fitting algorithm for the full potential equation', *AIAA 3rd Computational Fluid Dynamics Conf.*, New Mexico, June 1977.
32. M. Hafez, W. Whitlow and S. Osher, 'Improved finite difference method for transonic potential flows', *AIAA Paper 84-0092*, 1984.
33. K. Oswatitsch, *Gas Dynamics*, Academic Press, 1956.
34. M. Sichel, 'Structure of weak non-Hugoniot shocks', *Phys. Fluids*, **6,** 653–663 (1967).

35. G. Dulikravish, 'Artificial mass concept and transonic viscous flow equation', *First Army Conf. on Applied Mathematics and Computing*, Washington, DC, May 1983.
36. W. Habashi and M. Hafez, 'Finite element solutions of transonic flow problems', *AIAA J.*, **20,** 1368–1377 (1982).
37. M. Salas, Private communication.
38. M. Hafez and D. Lovell, 'Improved relaxation schemes for transonic potential calculations', *AIAA Paper 83-0372*, 1983.
39. A. Jameson, 'A multi-grid solution method for the Euler equations', *Int. Multigrid Conf.*, Copper Mountain, CO, 1983.